Journal of GeoEngineering, Vol. 17, No. 2, pp. 069-083, June 2022
http://dx.doi.org/10.6310/jog.202206_17(2).2

CALIFORNIA BEARING RATIO TEST ON REINFORCED CLAY UNDER AS-COMPACTED AND SOAKED CONDITIONS

Minh-Duc Nguyen [1*] and Kuo-Hsin Yang [2]

ABSTRACT

This paper presents a series of laboratory tests of the California bearing ratio (CBR) for investigating the bearing capacity and effects of the soaking process on the strength reduction of reinforced clay. Specimens were prepared using varying numbers of reinforcement layers, compaction energies, and soaking conditions. The results revealed that the CBR value significantly increased for specimens reinforced with nonwoven geotextile layers under soaked and unsoaked conditions. The maximum bearing capacity ratio of the reinforced clay was between 1.3 and 1.5 for the unsoaked specimens, which was lower than that of the soaked specimens (4.3 to 8.6). The soaking process induced a drastic decrease in the CBR value of unreinforced clay by up to 91.7%, which minimized to less than 68.8% when nonwoven reinforcement was used. The analysis of the CBR decrease as a result of wetting and swelling demonstrated that the CBR of unreinforced specimens decreased by approximately 80% under soaking without a change in density and could be further decreased to less than 50% using reinforcement with a nonwoven geotextile.

Key words: Geosynthetics, California bearing ratio, bearing capacity, reinforced soils, clays.

1. INTRODUCTION

The increasing demand for transportation development has led to more roads being constructed in the rural areas of the Mekong Delta region, Vietnam. For these projects, the use of riverbed clay excavated from the Mekong River as backfill soil is a cost-effective method. In addition to representing a green and sustainable development solution, other advantages include: (1) the avoidance of the environmental effects of the riverbed clay extracted through the dredging process, (2) reduction in the use of natural sand, and (3) decrease in the cost of construction. In the last 5 years, this principle was applied in laying the foundation of several roads using geosynthetic-reinforced clay. Figure 1 depicts a rural road composed of reinforced concrete pavement supported by a reinforced riverbed clay structure in Kien Giang Province, Vietnam. The riverbed clay was dried, compacted using layers, and reinforced through geotextile inclusion to improve its shear strength. The permeable nonwoven geotextile was chosen for the reinforcement layers because of its ability to significantly enhance the shear behavior of the reinforced clay (Ingold and Miller 1982; Fourier and Fabian 1987; Noorzad and Mirmoradi 2010; Mirzababaei *et al.* 2013; Yang *et al.* 2015; Yang *et al.* 2016). After construction, the road was stable and could only be traversed by vehicles with a load of less than 5 t. Although the shear strength of the clay was significantly improved after this treatment, the reinforced clay may suffer a severe shear strength reduction and expansion following saturation resulting from rainfalls and tides, which can cause road instability. Zornberg and Mitchell (1994) reported that the inherent low strength, moisture instability, possible volume changes, and creep potential represented additional concerns in regards to using marginal backfill. To remedy the disadvantages of marginal backfills, an appropriate drainage system for reinforced soil structures was applied, as suggested in other studies (Sridharan *et al.* 1991; Chen and Yu 2011; Taechakumthorn and Rowe 2012). However, the stability of the reinforced clay structure was questionable when soaked with water, requiring an in-depth analysis of both the bearing capacity and failure mechanism of these structural types under different conditions, including moisture content, reinforcement type, and arrangement.

To investigate the bearing capacity of reinforced clay, numerous studies have employed laboratory and in-situ tests for the California bearing ratio (CBR) because of its applicability to a wide range of different material and remold specimens. The CBR value is a common index property used to evaluate the strength of subgrade soil, subbase, and base course materials for determining the thickness of highways and airfield pavements. The CBR is also used to estimate the resilient modulus for characterizing the subgrade support for flexible and rigid pavements and determining structural layer coefficients for flexible pavements by using correlations provided in the design guidelines of the AASHTO (1993) and NCHRP (2014). The CBR results for reinforced soil demonstrated the bearing capacity improvement in clay specimens reinforced with geogrids (Moghaddas-Nejad and Small 1996; Kamel *et al.* 2004; Choudhary *et al.* 2012; Adams *et al.* 2016; Keerthi and Kori 2018; Singh *et al.* 2019) and geotextiles (Koerner *et al.* 1995; Carlo *et al.* 2016; Rajesh *et al.* 2016).

Based on the CBR values, the influence of the reinforcement arrangement on the bearing capacity of reinforced clay was also investigated. Using soil reinforced with a single reinforcement layer, Koerner *et al.* (1995) determined the CBR of the geosynthetic clay liners (GCLs) under a sand layer. The experimental results revealed that the most significant CBR improvement was exhibited in the GCL specimens with a sand layer thickness equal to that of the loaded piston diameter. Moghaddas-Nejad and Small (1996) concluded that placing the geogrid in the middle of

Manuscript received June 6, 2021; revised August 12, 2021; accepted February 17, 2022.
[1*] Ph.D. candidate (corresponding author), Faculty of Civil Engineering, Ho Chi Minh City University of Technology and Education, Ho Chi Minh City, Vietnam (e-mail: ducnm@hcmute.edu.vn).
[2] Professor, Department of Civil Engineering, National Taiwan University, Taipei, Taiwan.

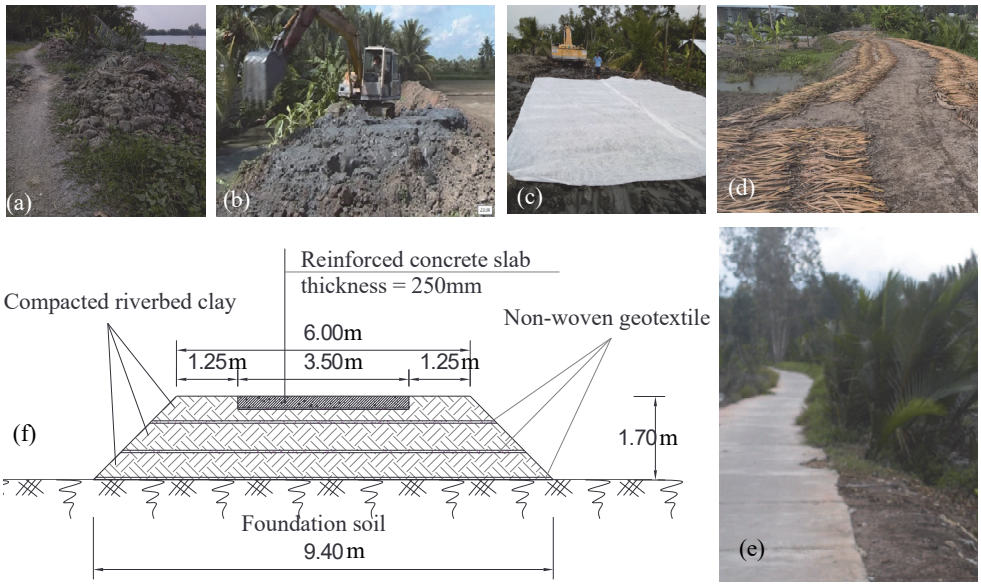

Fig. 1 Geotextile reinforced clay for rural road construction in Kien Giang Province, Vietnam: (a) before construction; (b) riverbed clay excavation; (c) compaction and reinforcement placement; (d) finish reinforced clay foundation; (e) completed road; and (f) cross-section design

the base layer was the most effective method for reducing the settlement of reinforced pavement. A similar observation was reported in Choudhary *et al.* (2012) and Keerthi and Kori (2018) when performing the CBR test on clay reinforced with either a single geogrid or jute textile layer. Singh *et al.* (2019) argued that the geosynthetic reinforcement layer must be placed either at mid-specimen-height or between the upper one-third and middle layers to achieve the highest bearing capacity. However, Kamel *et al.* (2004) asserted that the optimal location of a single geogrid layer was at 72% to 76% of the specimen height for three types of soil, namely clean sand, sandy clay, and clayey silt. Furthermore, the CBR values of clay reinforced using varying numbers of reinforcement layers have been investigated in other studies. Adams *et al.* (2016) observed that two-layer geogrid reinforcement only marginally improved the strength over single-layer reinforcement when placed close to mid-depth from the top of the compacted soil specimens. However, Carlo *et al.* (2016) performed the CBR tests by using a nonwoven geotextile with high-tenacity polyester yarns and reinforced fine soil under soaking conditions. The laboratory measurement demonstrated that the bearing capacity of the reinforced specimens was higher than that of the unreinforced samples; the higher the number of reinforcement layers, the higher the bearing capacity of the reinforced specimens. This bearing capacity improvement was attributed to tension membrane support, and the alternate surface failure enhancing the shear strength was attributed to the effect of the reinforcement layers.

The influence of water content on the bearing capacity of reinforced clay has been determined. Adams *et al.* (2016) and Lakshmi *et al.* (2016) have noted a drastic decrease in the CBR value of silty clay and lateritic soil after soaking, respectively. The bearing capacity of lateritic soil reinforced with a geogrid was also significantly reduced following soaking (Adams *et al.* 2016). For compacted clay, the behavior transited from brittle to plastic behavior when the water content was increased (Spangler and Handy 1973; Mitchell and Soga 2005; Holtz *et al.* 2011; Malizia and Shakoor 2018). Clayey soil immersed in water typically expands, reducing in density. Consequently, the bearing capacity reduction of clayey soil after soaking was derived from the increment of the water content (*i.e.,* wetting effect) and reduction in soil density as a result of soil expansion (*i.e.,* swelling effect). However, these two effects have not been not thoroughly analyzed in relation to the bearing capacity reduction of reinforced clay following saturation.

In this study, a series of laboratory tests was performed to examine the CBR behavior of clay reinforced with a nonwoven geotextile under soaked and unsoaked conditions. The method for estimating the actual thickness of the geotextile layers embedded in the compacted specimens was proposed by Nguyen *et al.* (2020) and was adopted in this study to determine the soil density in the reinforced specimens following compaction. The objectives of this study were: (1) to examine the reinforcing effect in terms of CBR improvement and density of reinforced clay under soaked and unsoaked conditions, and (2) to estimate the influence of the swelling and wetting effect on the bearing capacity of reinforced clay. The obtained results provide useful information for the use of nonwoven geotextiles for improving the bearing capacity of reinforced clay structures.

2. EXPERIMENTAL PROGRAM

A total of 30 laboratory tests were conducted to determine the CBR value of clay reinforced with a nonwoven geotextile. Variations in the test included the number of reinforcement layers, compaction energy levels, and soaking conditions.

2.1 Test Materials

2.1.1 Riverbed Clay

Kien Giang riverbed clay was excavated from the riverbed of Cai Lon River in the Mekong Delta, Vietnam. The clay is classified as high plastic inorganic silt as per the Unified Soil Classification System. The properties of the soil are listed in Table 1. The potential swelling behavior of the Kien Giang riverbed

Table 1 Soil properties

Unified Soil Classification System		MH	
Plastic limit, PL (%)		44.9	
Plastic index, PI (%)		46.6	
Liquid limit, LL (%)		91.5	
Specific gravity, G_s		2.75	
Free swell index (%)		55.9	
Modified Proctor compaction test			
Compaction energy, E (kJ/m^3)	Total number of blows	OMC (%)	Maximum dry unit weight (kN/m^3)
482	50	26.6	13.61
1,200	125	24.5	15.11
2,700	280	20.5	16.15

clay was determined using the free swell index test following IS: 2720-40. Following a measure of 55.9% using the free swell index, the soil was classified as medium expansive soil (IS: 1498). The modified Proctor test following ASTM D1557 was applied to determine the optimum moisture content (OMC) and maximum dry unit weight of the clay, which would be used later for preparing specimens in the CBR test. With a mold 15.24 cm in diameter, 116.6 mm in height, and with a modified Proctor rammer (44.48 N drop from 457.2 mm), the soil specimens were compacted using six layers instead of five layers specified in ASTM D1557. The number of compaction layers was modified to adapt to the reinforcement arrangement of the reinforced specimens. The number of blows per compaction was also estimated in correspondence to the three compaction energy levels (E) 2700, 1200, and 482 kJ/m^3, as suggested in ASTM D1883. The maximum dry unit weight and OMC for each compaction energy level were evaluated and are summarized in Table 1. The results indicated that a high E value induced an increase in the maximum dry unit weight and decrease in the OMC.

Using the same clayey soil, Nguyen *et al.* (2021) investigated its shear strength of the clay by the direct shear test. The coheshion and friction angle of the clay under as-compacted conditions were 96.0 kPa and 26.4°, whereas under saturated conditions were 45.5 kPa and 18.6°, respectively. That awareble shear strength loss of compacted clay after saturation was caused by the loss of suction of the soils with the increase in moisture content and the possible development of excess pore water pressure in saturated clays, which reduces the effective stresses and the shear resistance (Abu-Farsakh *et al.* 2007).

2.1.2 Geotextile

A commercially available needle-punched polyethylene terephthalate nonwoven geotextile was used, the properties of which are presented in Table 2. This geotextile had a permittivity of ψ equal to 1.96 s^{-1}, and corresponding cross-plane permeability of k equal to 3.5×10^{-3} m/s which is higher than the permeabilty of the compacted clay. The load-elongation behavior of reinforcement was determined using the wide-width tensile test in the longitudinal and transverse directions (Nguyen *et al.* 2013). The experimental results revealed the anisotropic tensile behavior of the geotextile.

The interface shear strength between the clay and the nonwoven geotextile under both as-compacted and saturated conditons were tests by Nguyen *et al.* (2021) and summarized in Table 3. The interface shear strength was significantly reduced after soil saturation. In particular, the interface shear strength

Table 2 The properties of nonwoven geotextile

Property	Value		
Fabrication process	Needle-punched PET nonwoven geotextile		
Mass (g/m^2)	200		
Thickness (mm)	1.78		
Apparent opening size (mm)	0.11		
Permittivity (s^{-1})	1.96		
Cross-plane permeability (m/s)	3.5×10^{-3}		
Wide-width tensile test			
Direction	Ultimate strength (kN/m)	Failure strain (%)	Secant stiffness @ peak value (kN/m)
Longitudinal	9.28	84.1	11.03
Transverse	7.08	117.8	6.01

Table 3 The interface shear strength of nonwoven geotextile and clay compacted using standard Proctor compaction energy, E = 600 kJ/m^3 (after Nguyen *et al.* 2021)

Water content	Interface shear strength		Efficiency factor, R_f	
	Cohesion (kPa)	Friction angle (°)	Range	Average
Optimum moisture content	40.1	22.1	0.41 ~ 0.68	0.59
Consolidation in the saturated condition	23.5	20.5	0.56 ~ 0.94	0.82

reduced about 13.4% ~ 27.7%, which was only 1/3 ~ 1/2 that of the compacted clay. The efficiency factor is defined as the ratio of the interface shear strength to the shear strength of clay. It was observed that the high efficiency factor at saturated conditions because the high permeable nonwoven geotextile enhanced the dissipation of excess porewater pressure of clay.

2.2 Specimen Preparation

A natural clay sample excavated from the riverbed in the form of wet bulk was dried in an oven (the temperature was set at less than 60°C) for a minimum of 24 h and then crushed and ground into powder using a mortar. Moisture soil specimens were prepared through mixing different quantities of clay powder and water corresponding to the desired optimum moisture listed in Table 1; they were then stored and sealed in a plastic bag in a temperature-controlled chamber for a minimum of 2 days to ensure a uniform distribution of moisture within the soil mass.

Since the geotextile layers only helped to improve the density of the soil without influencing the optimum moisture content (Nguyen *et al.* 2020), both the unreinforced and reinforced specimens were prepared using the clay at the same optimum moisture content in a mold with a diameter (D) of 152.4 mm and height of 116.6 mm. They were compacted using the modified Proctor rammer in six compaction layers. For the unreinforced specimens, the number of blows and the amount of soil per compaction layer were evaluated using the results of the modified Proctor compaction test. The total amount of soil used must be such that the last compacted layer extends into the collar slightly but not by more than approximately 6 mm above the top of the mold, as stated in ASTM D1557. Before removal of the collar, the soil adjacent to the collar was cut to loosen it from the collar and avoid disrupting the soil below the top of the mold. The compacted specimen was trimmed for evenness with the top of

the mold using a knife. Any holes in the top surface were filled with uncompacted soil and pressed in by hand; then, a straight edge was scraped across the top of the mold. After the soil specimens were compacted, their moisture weight W and water content ω were measured.

The dry unit weight of the unreinforced specimens $\gamma_{d\text{-}unre}$ was calculated as

$$\gamma_{d\text{-}unre} = \frac{W}{(1+\omega)V} \quad (1)$$

where V represents the mold volume.

The reinforced specimens were also compacted using six compaction layers but stabilized with one, two, three, and five reinforcement layers (Fig. 2). After each soil layer was compacted and leveled, the soil surface was scarified before a 152.4-mm-diameter dry geotextile layer was placed horizontally on the roughened surface. The required amount of soil for the next layer was then poured and compacted. The process for constructing the surface of the reinforced specimens was similar to that of the unreinforced specimens. The procedure to prepare the reinforced specimens was followed to that proposed by Nguyen *et al.* (2020). Also adapted from Nguyen *et al.* (2020), the dry unit weight of the reinforced soil $\gamma_{d\text{-re}}$ was measured using the pure soil compacted between the geotextile layers of the reinforced soil rather than the overall specimen with the inclusion.

$$\gamma_{d\text{-re}} = 4\frac{W_{\text{re}} - W_{\text{geo}}}{\pi D^2\left(H - \sum_{i=1}^{n} t_i\right)(1+\omega)} \quad (2)$$

where W_{geo}, W_{re} are the dry weight of all the reinforcement layers and the moisture weight of the reinforced specimens, respectively; i and n denote the ordinal number and total number of reinforcement layers in the reinforced specimens, respectively; and t_i represents the actual thickness of the reinforcement layer i in the compacted specimens. The dry unit weight of the specimens was calculated and is listed in Table 4.

To produce the soaked specimens, the compacted specimens were immersed for 96 h prior to the CBR test. The surface of the specimens was loaded using a 4.54 kg mass surcharge, following which the mold and weights were immersed in tap water, allowing the water free access to the top and bottom of the specimen (ASTM D1883). During the soaking process, the swell of the specimens was recorded each 1 to 2 h.

2.3 Testing Program

The laboratory test for the CBR value was performed following the ASTM D1883 instructions. The same surcharge mass (4.54 kg) was placed on the specimens before application of the load on the piston with a diameter (b) of 49.7 mm, which penetrated the specimens. The ratio between the diameter of reinforcement and piston D/b in this study was approximately 3.1, which is slightly less than the optimal range of 3.15 to 3.80 proposed by Chakraborty and Kumar (2014) for obtaining the highest bearing capacity for a circular reinforced foundation. This ratio is also less than that of the strip and square foundation, which was approximately 6 to 8 and 4.5, respectively (Khing *et al.* 1993; Omar *et al.* 1993).

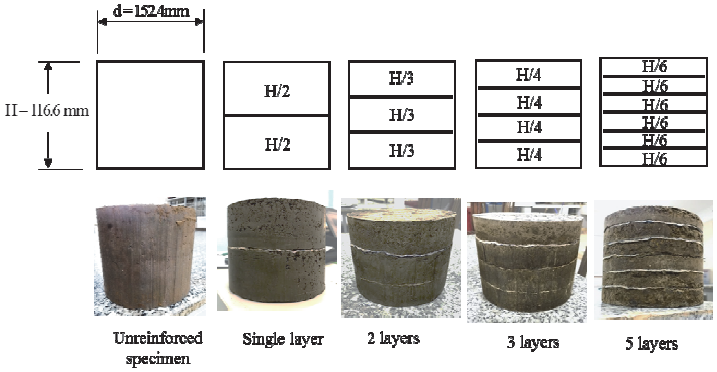

Fig. 2 Geotextile arrangement in specimens

Table 4 CBR values, dry unit weights, and percent dry unit weight reductions of specimens due to soaking with fractional error

Cases	Compaction energy, E (kJ/m^3)	Dry unit weight (kN/m^3)	CBR of unsoaked specimens (%)	CBR of soaked specimens (%)	Percent dry unit weight reduction, $\%\Delta\gamma_d$ (%)	Fractional error, % (*)
Unreinforced	482	13.61	9.5	1.5	4.21	
1 layer	482	13.71	12.3	5.0	4.08	0.216
2 layers	482	13.94	14.2	6.6	3.98	0.317
3 layers	482	14.47	11.7	5.0	3.58	0.397
5 layers	482	14.66	10.8	3.4	3.43	0.532
Unreinforced	1,200	15.11	17.3	2.7	4.51	
1 layer	1,200	15.19	19.3	9.0	4.18	0.212
2 layers	1,200	15.25	24.7	12.7	4.11	0.315
3 layers	1,200	15.80	19.8	9.1	3.69	0.394
5 layers	1,200	16.06	18.5	7.1	3.52	0.531
Unreinforced	2,700	16.15	40.1	3.4	5.21	
1 layer	2,700	16.23	44.2	19.5	4.84	0.211
2 layers	2,700	16.38	51.8	29.6	4.77	0.313
3 layers	2,700	16.71	45.9	16.5	4.58	0.392
5 layers	2,700	16.86	43.1	13.5	4.46	0.526

(*) the fractional error was only applicable for reinforced specimens only

The rate of penetration of the piston was approximately 0.05 in/min (1.27 mm/min), and the tests were halted when at a penetration diameter of 20 mm. In most cases, the zero point of the stress–penetration curves was adjusted owing to surface irregularities or other causes, as recommended in ASTM D1883. Consequently, the corrected penetration of the tests would be less than the actual penetration of the piston at the end of the tests (Figs. 8 and 9).

The CBR value can be obtained as follows:

$$CBR_1(\%) = \frac{P_1}{6900} \times 100 \tag{3}$$

$$CBR_1(\%) = \frac{P_2}{10300} \times 100 \tag{4}$$

P_1 and P_2 are the kPa stresses on a piston at 2.54 and 5.08 mm after corrected penetration, respectively. The CBR value is typically chosen as the higher value of CBR_1 and CBR_2. In general, CBR_1 is higher than CBR_2, and the CBR is equal to CBR_1. If CBR_2 is greater than CBR_1, CBR_2 is chosen as the CBR value after the redo tests verify the accuracy of the original test result (ASTM D1883).

2.4 Estimating the Actual Thickness of the Geotextile Layer in Compacted Specimens

As proposed by Nguyen *et al.* (2020), the actual thickness of the reinforcement layer in the reinforced soil was reduced from its undeformed thickness as a result of the dynamic forces from the rammer blows during compaction and overburden pressure of the soil layer above after compaction. The average of the upper bound value t_{max} (*i.e.,* maximum thickness value) and lower bound value t_{min} (*i.e.,* minimum thickness value) could be determined. The t_{max} was the thickness of the geotextile layers under the overburden pressure $q_{overburden}$ of the above soil layer without compaction, and the t_{min} value was the thickness under the $q_{overburden}$ after the compaction test was performed on the geotextile layers without soil. The compaction energy of the test was the same as that of the compacted reinforced specimens. The thickness of the geotextile layer compacted without soil was less than the actual thickness of the geotextile in the compacted specimens, which is attributable to the shorter distance the rammer travels to reach the reinforcement layers during impact compared with the distance it travels to reach the reinforced specimens. The actual thickness of the reinforcement layer i in the reinforced compacted specimens was calculated as the mean value of t_{max} and t_{min} (Nguyen *et al.* 2020).

The $q_{overburden}$ acting on the geotextile layer is expressed as

$$q_{\text{overburden}} = d_i \gamma \tag{5}$$

where d_i is the depth of the geotextile layer i in the specimens after compaction, and γ is the bulk unit weight of thecompacted soil. In the reinforced specimens, the top and bottom layers were assigned as the first layer, $i = 1$, and last layer, $i = n$, respectively, in which n denotes the total number of reinforcement layers.

The error of $\gamma_{d\text{-re}}$ caused through the evaluation of t_i could be analyzed using the following factional error proposed by Nguyen *et al.* (2020):

$$\frac{\sigma_{\gamma d\text{-re}}}{\gamma_{d\text{-re}}} = \frac{\sqrt{\sum_{i=1}^{n} \sigma_{ti}^2}}{H - \sum_{i=1}^{n} t_i} \tag{6}$$

in which σ_{ti} represents the standard deviation of the geotextile thickness σ_{ti}.

$$\sigma_{ti} = \frac{t_{\max} - t_{\min}}{2} \tag{7}$$

As presented in Table 4, the fractional error $\sigma_{\gamma d\text{-re}}/\gamma_{d\text{-re}}$ was less than 0.6% for all cases and was thus suitable for evaluating the thickness of the reinforcement layers in the reinforced soil following compaction.

3. RESULTS AND DISCUSSION

3.1 Influence of the Nonwoven Geotextile on the Swell Behavior of Reinforced Clay

As a medium expansive soil, the volume of the unreinforced and reinforced specimens increased under soaking. Because the nonwoven geotextile is an inert material and the total thickness of the reinforcement layers is much smaller than that of the soil in the reinforced specimens (more than 14 times difference), the thickness of the reinforcement layers after soaking changed non-significantly, and the swell of the reinforced specimens mainly resulted from the expansion of the clay. The swells of all of the specimens (both unreinforced and reinforced specimens) during soaking were quantified using the percent swell S, in which only the soil swell was considered.

$$S = \frac{s}{H_{\text{soil}}} \times 100\% \tag{6}$$

where s is the vertical swell measured with time, and H_{soil} denotes the total height of the soil in the specimens (excluding the thickness of the reinforcement layers, if any) before soaking.

$$H_{\text{soil}} = H - \sum_{i=1}^{n} t_i \tag{7}$$

The variations of the percent swell of the unreinforced and reinforced specimens over time are illustrated in Fig. 3. The percent swell tended to increase with time and did not reach equilibrium within 96 h of soaking. A similar finding was reported in Al-Taie *et al.* (2016), in which the maximum swell-shrink also failed to occur after the first 96-h soaking cycle.

Owing to the permeability of the nonwoven geotextile, the swell behavior of the reinforced specimens differed from that of the unreinforced specimens. During the initial period of soaking, the percent swell of the unreinforced specimens was less than that of the reinforced specimens. However, gradually, the accumulated swell of the unreinforced specimens exceeded that of the reinforced specimens. After 96 h, the percent swell of the reinforced specimens decreased when the number of reinforcement layers was increased (Fig. 3) as a result of the effectof soil-reinforcement interaction inducing local lateral confinement in the reinforced specimens. As detailed in Choudhary *et al.* (2012), the expansion in soil develops in all

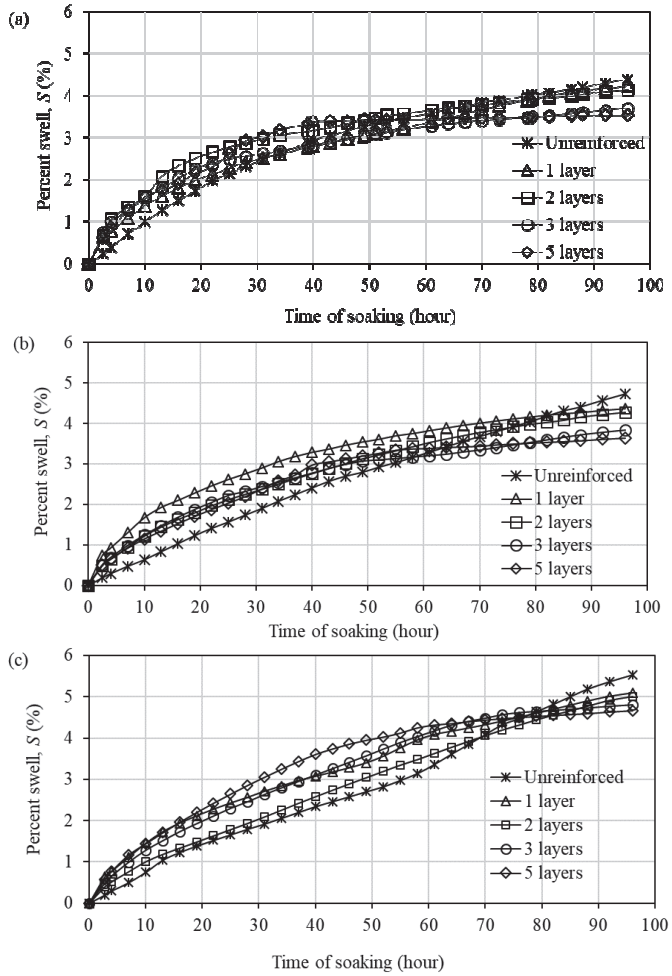

Fig. 3 Percentage of swelling of unreinforced and reinforced specimens compacted by different compaction energy levels: (a) 482 kJ/m^3; (b) 1,200 kJ/m^3; and (c) 2,700 kJ/m^3

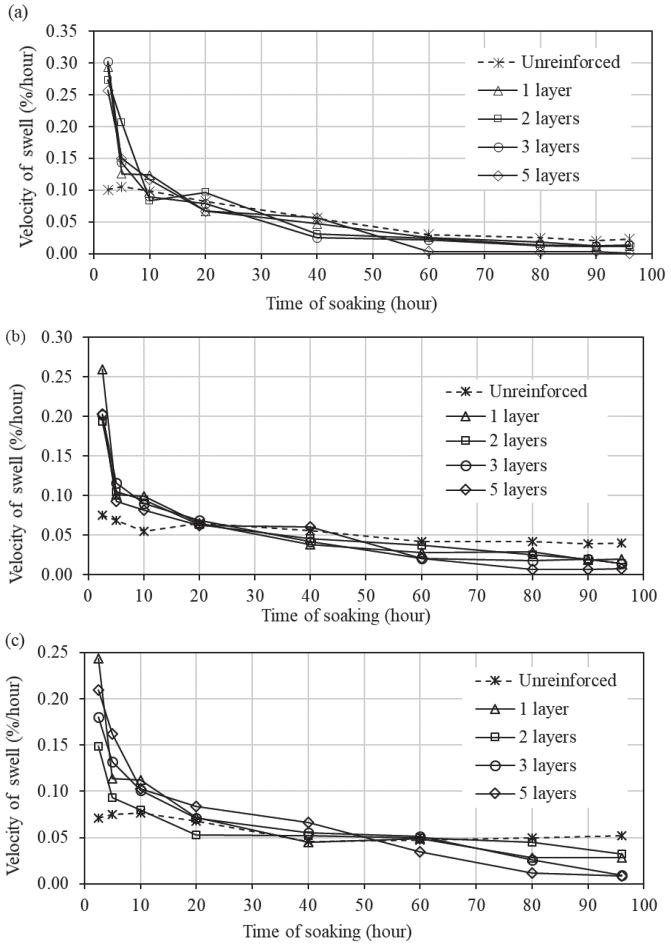

Fig. 4 Velocity of swell in the unreinforced and reinforced specimens compacted by different compaction energy levels: (a) 482 kJ/m^3; (b) 1,200 kJ/m^3, and (c) 2,700 kJ/m^3

directions, mobilizing the interfacial frictional force between the soil and form of reinforcement. This frictional force tends to counteract the swelling pressure in a direction parallel to reinforcement and consequently reduces the heave of the soil (Keerthi and Kori 2018). For the specimens reinforced with five geotextile layers, the percent swell decreased by between 0.9% and 1.1% compared with that of unreinforced specimens following 96 h of soaking. Consequently, the soil density reduction of the reinforced specimens was smaller, which minimized the loss of strength of the reinforced clay after soaking. The reduction of bearing capacity resulting from soaking was further evaluated using the CBR value results of the unreinforced and reinforced specimens.

The swelling velocity, defined as the percent swell of the specimens/h, was also assessed to illustrate the influence of reinforcement on the swell behavior of the reinforced specimens. As depicted in Fig. 4, the swell velocity of the reinforced specimens was higher than that of the unreinforced specimens within the first of 10 to 20 h of soaking. In the first 2.5 h, the swell velocity of the reinforced specimens was 0.25% to 0.3%/h, 2.5 to 3 times that of the unreinforced specimens. This resulted from the increment of the drainage paths of the nonwoven geotextile layers in the reinforced specimens. As a permeable material, the reinforcement layers could not prevent the intrusion of water into the reinforced specimens. Following 10 h of soaking, the swell velocity of the reinforced specimens decreased drastically to a value as small as that of the unreinforced specimens and continued to decrease; after 60 h, the swell velocity of the reinforced soil was less than that of the unreinforced soil. After 96 h, the higher the number of reinforcement layers, the lower the swell velocity was. That is, the swell of specimens reinforced with a higher number of reinforcement layers achieved equilibrium more rapidly with a lower total percent swell.

By contrast, at the beginning of soaking, the swell velocity of the unreinforced soil was low, approximately 0.07% to 0.1%/h, and gradually decreased over time. After 96 h, the swell velocity remained as high as 0.2% to 0.5%/h, and the total swell of the unreinforced specimens continued to increase, particularly those compacted using 1,200 and 2,700 kJ/m^3, as presented in Figs. 4(b) and 4(c), respectively. In short, the nonwoven geotextile layers induced a rapid increase in swell and decreased total percent swell in the reinforced clay after soaking.

3.2 Density of Unreinforced and Reinforced Specimens After Compacting and Soaking

Figure 5 illustrates the variation of the percent swell with the

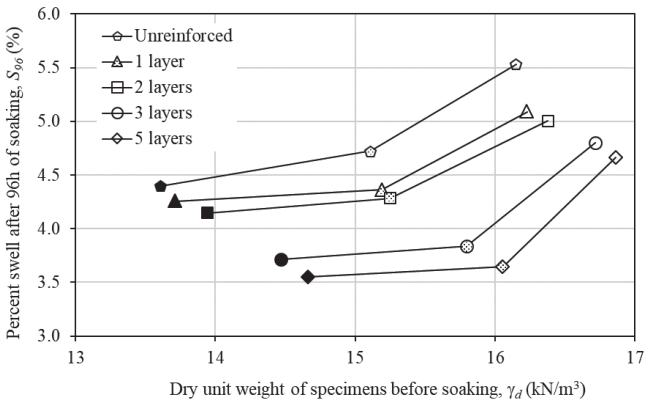

Fig. 5 Variation of percent swells after 96 hours of soaking with dry unit weights of unreinforced and reinforced specimens. The bold, dot, and empty nodes exhibit the specimens compacted by 482, 1,200, and 2,700 kJ/m³ of compaction energy level, respectively.

dry unit weight of the unreinforced and reinforced clay specimens before soaking, which had increased. A similar observation had been observed in compacted fine-grained soils and highly consolidated clay in Sridharan and Gurtug (2004) and Khemissa *et al.* (2018), respectively.

Table 4 exhibits the effect of reinforcement on improving the compaction density of the reinforced specimens after compaction. Under the three compaction energy levels (482, 1200, and 2700 kJ/m³), the dry unit weight of the reinforced specimens was greater than that of the unreinforced specimens. The increment of the number of reinforcement layers induced a higher density in the reinforced specimens after compaction and thus enhanced the compaction effectiveness in densifying the reinforced clay. The obtained results corroborate those of several studies (Indraratna *et al.* 1991; Keskin *et al.* 2009; Nguyen *et al.* 2020) that evaluated the dry unit weight of soil only after deducting the dry weight and volume of reinforcement layers from reinforced specimens. The density improvement of the reinforced soil following compaction was explained as the enhanced dissipation of excess pore-water pressure and high air permeability of the nonwoven geotextiles as well as the restrained expansion of the soil between the reinforcement layers under compaction forces (Nguyen *et al.* 2020).

One of the consequences of soaking is reduced soil density. During the soaking process, the dry weight of the soil specimens remained unchanged, but their volume increased through swelling. The dry unit weight of the soil specimens then decreased after soaking. Figure 6 presents the relationship between the dry unit weight of the unreinforced and reinforced specimens before and after 96 h of soaking. The dry unit weight of the soaked specimens was lower and strongly correlated with the unsoaked specimens (R^2 = 0.994). A linear function regressed from the relationships between these two values was constructed and later used to distinguish the dry unit weight of the soaked specimens from that of the equivalent unsoaked specimens. The density reduction of the specimens following 96 h of soaking was evaluated using the percentage of dry unit weight reduction of the soil $\%\Delta\gamma_d$ as follows:

$$\%\Delta\gamma_d = \frac{\gamma_{d\_\text{unsoaked}} - \gamma_{d\_\text{soaked}}}{\gamma_{d\_\text{unsoaked}}} \times 100\% \quad (8)$$

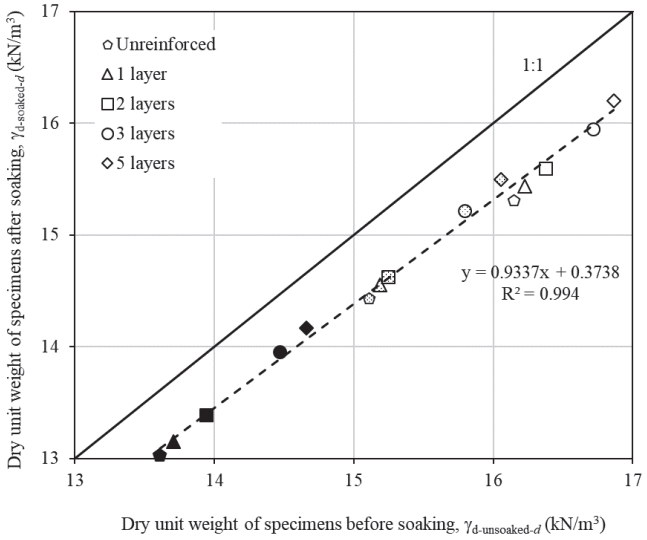

Fig. 6 Comparison of dry unit weight of unreinforced and reinforced specimens before and after 96 hours of soaking. The bold, dot, and empty nodes exhibit the specimens compacted by 482, 1,200, and 2,700 kJ/m³ of compaction energy level, respectively.

where $\gamma_{d\_\text{unsoaked}}$ and γ_{d_soaked} are the dry unit weights of a specimen before and after 96 h of soaking, respectively.

Because the changes in the thickness of the reinforcement layers in the reinforced specimens after soaking were marginal, the value of $\%\Delta\gamma_d$ was calculated using the percent swell after 96 h of soaking S_{96}.

$$\%\Delta\gamma_d = 1 - \frac{1}{S_{96} + 1} \quad (9)$$

Table 4 lists the percentage of dry unit weight reduction of the unreinforced and reinforced clay specimens after soaking of the specimens for 96 h. The larger the number of reinforcement layers, the lower the reduction of the dry unit weight of the soil. Compared with the unreinforced clay specimens, a smaller dry density reduction (by 0.8% to 1%) was observed in the specimen reinforced using five reinforcement layers. This observation is consistent with the swelling characteristics of needle-punched, thermally treated GCLs. Lake and Rowe (2000) noted that reinforced GCLs provide additional confinement to the bentonite, which may prevent swelling of the bentonite during hydration. In the nonwoven geotxtile reinforced clay, a high efficiency factor would enable to mobilize high reinforcement tension to confine the clay swelling when soaking (Table 3).

In summary, the high permeable nonwoven geotextile layers not only improved the density of the reinforced clay specimens after compaction but also confined the expansion of the clay to mitigate the density reduction when soaking. The later was activated by a good interface interfaction between saturated clay and reinforcement layers. These effects increased with the increment of the number of reinforcement layers. Consequently, after soaking, the dry unit weight of the reinforced specimens was significantly higher than that of the unreinforced specimens, which assisted in clarifying the process of the bearing capacity improvement of the soaked reinforced specimens.

3.3 CBR Behavior of Unreinforced and Reinforced Specimens with a Geotextile Under Unsoaked and Soaked Conditions

Figures 7 and 8 depict the variation of the stress on the piston of the unsoaked and soaked specimens with the corrected penetration, respectively. For the specimens with and without soaking, the bearing capacity was significantly improved when reinforced with nonwoven geotextile layers. A similar finding has been reported in numerous studies (Abduljauwad *et al.* 1994; Koerner and Narejo 1995; Kamel *et al.* 2004; Choudhary *et al.* 2012; Adam *et al.* 2016; Carlos *et al.* 2016; Rajesh *et al.* 2016; Keerthi and Kori 2018; Singh *et al.* 2019). These researchers have concluded that the reinforcement layers improved the CBR value of reinforced soil.

Additionally, for unsoaked specimens, when the penetration depth was less than 10 to 12 mm, the corrected penetration of the specimens reinforced with two layers was the highest value. However, gradually, with the penetration increment, the specimens reinforced with five reinforcement layers achieved a higher bearing capacity (Fig. 7) at a penetration of 18 mm.

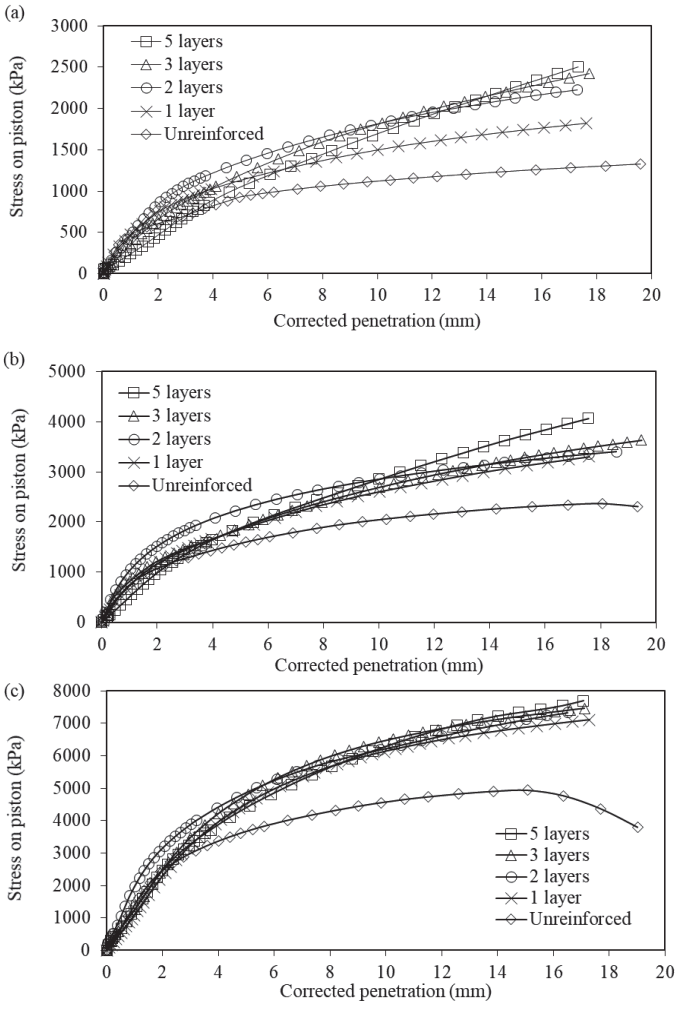

Fig. 7 Stress on piston of unsoaked specimens compacted by 3 different compaction energy levels: (a) 482 kJ/m^3; (b) 1200 kJ/m^3; (c) 2700 kJ/m^3

For the soaked specimens, the bearing capacity of the specimens reinforced with two reinforcement layers was much higher than that of the other specimens when the penetration was less than 18 mm. Beyond 18-mm piston penetration, the specimens reinforced with five layers exhibited the highest bearing capacity (Fig. 8). However, in regards to the reinforced specimens compacted using an E of 2,700 kJ/m^3, after soaking, the stress-penetration exhibited softening behavior, of which the maximum bearing capacity did not change in accordance with the number of reinforcement layers as expected.

The improvement of the bearing capacity of the reinforced specimens was attributed to the soil-reinforcement interaction in the reinforced specimens. The reinforcement layers acted to restrain the lateral deformation resulting from the interfacial shear stress between the soil and reinforcement. The tension membrane developed an upward force inducing an increase in the bearing capacity, manifesting in the concave deformation in the reinforcement layers of the reinforced specimens after the tests. These reinforcing mechanisms have been described by Giroud and Noray (1981), Chen and Abu-Farsakh (2015), and Carlos *et al.* (2016).

At a low penetration, the reinforcement deformation was slight, and the confinement effect enhanced the bearing capacity. The bearing capacity of the reinforced specimens depended heavily on the depth of the top reinforcement layer d_1. Chakraborty and Kumar (2014) also identified a critical depth of

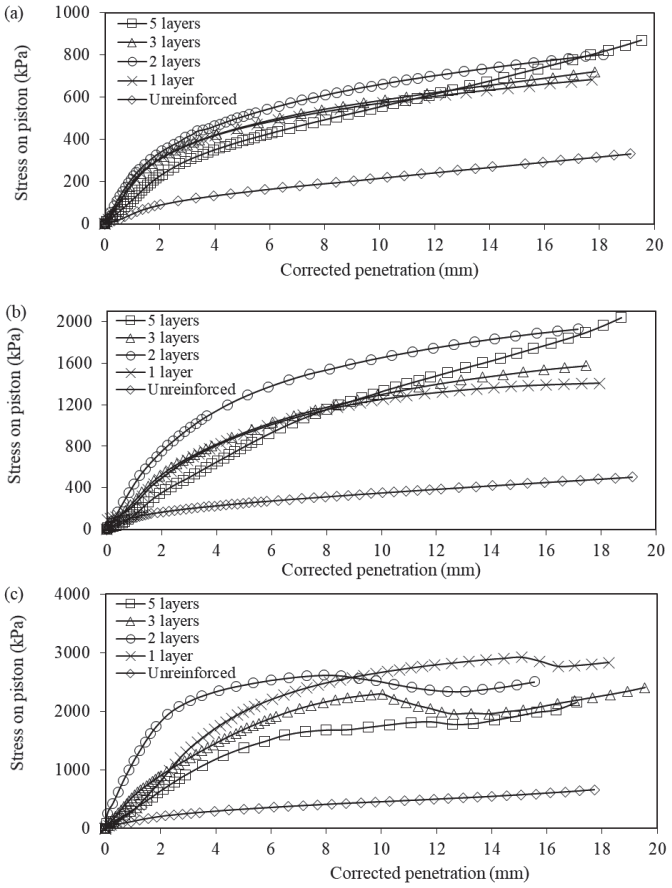

Fig. 8 Stress on piston of soaked specimens compacted by 3 different compaction energy levels: (a) 482 kJ/m^3; (b) 1200 kJ/m^3; (c) 2700 kJ/m^3

the top reinforcement sheet for achieving the highest bearing capacity of circular reinforced foundations. As presented in Table 4, the CBR value of the reinforced specimens was much higher than that of the unreinforced specimens, with that of the specimens reinforced with two reinforcement layers reaching the highest value. Therefore, the optimal value of d_1 for attaining the highest CBR value of the reinforced specimens in this study was 38.8 mm (d_1/b = 0.78).

Different optimal values for d_1/b have been reported in other studies, which was might caused by the differences in soils, reinforcement materials, and boundary conditions. For example, Koerner and Narejo (1995) determined that the soil thickness required to cover a GCL must be at least equal to the diameter of the load piston (*i.e.,* d_1/b = 1). A similar conclusion has been presented in Choudhary *et al.* (2012) and Keerthi and Kori (2018) following conduction of CBR tests on expansive soil subgrades reinforced with a single reinforcement layer. However, Kamel *et al.* (2004) observed that a geogrid layer placed at a depth of approximately 1 to 1.2 times the diameter of the plate load attained the highest CBR value among reinforced specimens. That optimal location of the top reinforcement layer was obtained through an investigation of the bearing capacity of the specimen reinforced with a single reinforcement layer, which would differ from that of soil reinforced using multiple reinforcement layers (Yetimoglu *et al.* 1994). In the case of a higher number of reinforcement layers, Carlos *et al.* (2016) noted that increasing the number of reinforcement layers from one to two led to the higher CBR behavior of the geosynthetic-reinforced fine soil, which was also reported in Singh *et al.* (2019).

The penetration caused concave-shaped deformation in the reinforcement layers, which enhanced the bearing capacity resulting from the tension membrane in the reinforcement layers (Carlos *et al.* 2016). When the penetration was sufficient, the upward force from the tension membrane was mobilized from the top and bottom reinforcement layer. It is justified by the concave shape of reinforcement layers was found after peeling off the upper soil layer to uncover the embedded reinforcement layer in the reinforced specimens after the CBR tests. Consequently, the higher the number of reinforcement layers, the greater the bearing capacity improvement. As illustrated in Figs. 7 and 8, when the penetration reached a specific value, the bearing capacity of the specimen reinforced with five reinforcement layers was the highest. That behavior was not observed in the soaked reinforced specimens compacted using an E of 2700 kJ/m^3 (Fig. 8(c)). Apart from the stress-penetration hardening behavior of the other specimens, these reinforced specimens exhibited stress-penetration softening behavior, in which the corrected stress increased to a peak value at approximately 10 to 16 mm of penetration, then gradually decreased. After the test, the reinforced specimens were dismantled, revealing that the topsoil layer was cracked radially and detached from the specimens, particularly from those reinforced with three and five reinforcement layers (Fig. 9); the high density of the soil may have caused brittle deformation. The shallow depth of the top reinforcement layer (*i.e.,* a high number of reinforcement layers) then triggered the detachment of the topsoil layer from the specimens at an adequate piston penetration. Therefore, the higher the number of reinforcement layers, the more vulnerable the topsoil, and the lower the bearing capacity at high piston penetration. It should be noted that the rupture of the reinforcement

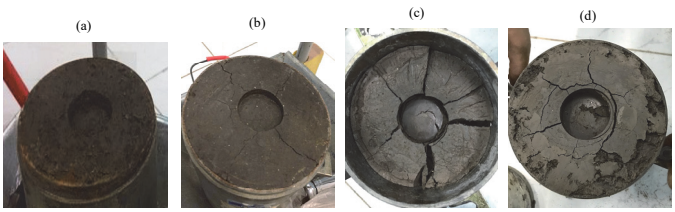

Fig. 9 Failure pattern of unreinforced: (a) soaked specimen; (b) unsoaked specimen and specimens with five reinforcement layers: (c) soaked specimen; and (d) unsoaked specimen. All of the specimens were compacted using 2700 kJ/m^3 of compaction energy level

layers was not found in any reinforced specimens after the CBR test, which ensured the tensile mobilization in reinfocement layers under a high deformation of reinforced specimens.

In short, the geotextile reinforcement enhanced the bearing capacity of the reinforced clay specimens both before and after soaking. At a low piston penetration (*i.e.,* less than 10 to 12 mm), the bearing capacity and CBR value reached their peak when the specimens were reinforced with two reinforcement layers. At up to 18 mm of piston penetration, the increment of the number of reinforcement layers induced an increment in the bearing capacity of the reinforced soil.

3.4 Bearing Capacity Ratio and Difference

The effects of reinforcement layers on enhancing the bearing capacity of reinforced clay are further discussed in this section. Figure 10 depicts the variations of the bearing capacity ratio (*BCR*) of the soaked and unsoaked specimens with the ratio of reinforcement spacing and diameter of piston, h/b and compaction energy levels. The *BCR* was defined as the ratio of the *CBR* value of the reinforced and unreinforced specimens when the two specimens were compacted using the same compaction energy. The *BCR* of the soaked specimens was much higher than that of the unsoaked specimens, the highest of which was only approximately 1.3 to 1.5; the peak *BCR* of the soaked specimens was 4.3 to 8.6. Additionally, the *BCR* of the soaked specimens increased with the increment of the compaction energy.

Other studies have reported different *BCR* values for soaked and unsoaked specimens. Regarding clay specimens reinforced with a single geogrid layer, Rajesh *et al.* 2016 concluded that the *BCR* of the unsoaked specimen was higher than that of the soaked specimens. By contrast, after soaking, the *BCR* of lateritic soil reinforced with one or two geogrid layers can increase or reduce depending on the type of soil and reinforcement arrangement (Adam *et al.* 2016).

The effectiveness of the nonwoven geotextile on improving the bearing capacity of reinforced specimens was also quantified using the bearing capacity difference ΔP. This was defined as the difference between the corrected stress of reinforced soil and that of unreinforced specimens at a piston penetration of 5.08 mm under the same compaction energy. Similar to the CBR value, the bearing capacity difference was evaluated using the corrected stress at 2.54-mm or 5.08-mm penetration. However, the corrected stress at the higher penetration was higher, and the evaluation of the ΔP using the bearing capacity of specimens at 5.08-mm piston penetration was preferred. As shown in Fig. 11, the bearing capacity difference reached its peak value in the

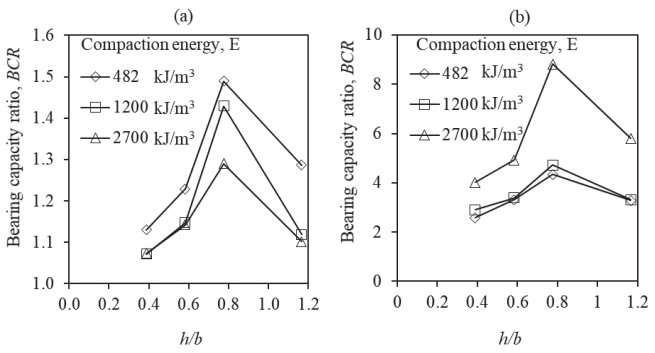

Fig. 10 Bearing capacity ratio of reinforced specimens compacted by 482, 1200, and 2700 kJ/m³ of compaction energy: (a) unsoaked specimens; (b) soaked specimens

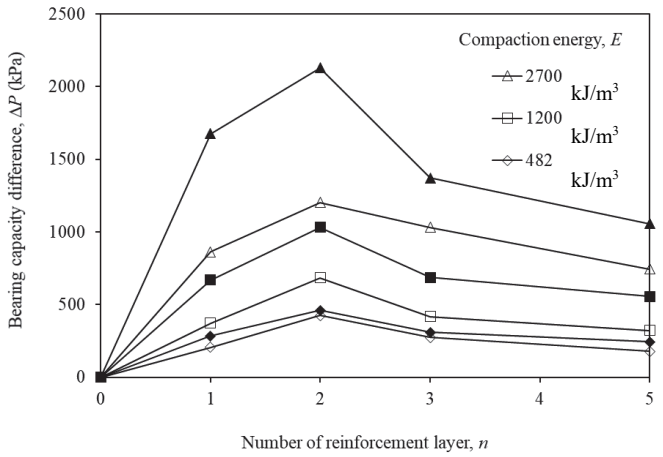

Fig. 11 Bearing capacity difference of specimens reinforced with different reinforcement layers. The empty and bold nodes indicate the values of unsoaked and soaked specimens, respectively.

specimens with two reinforcement layers, which is consistent with the results of the *BCR*. For both the soaked and unsoaked specimens, the value of ΔP increased with the increased compaction energy, with greater bearing capacity improvement obtained when the reinforced clay was compacted using a high compaction energy.

Furthermore, similar to the *BCR*, the bearing capacity difference of the soaked reinforced specimens was higher than that of the unsoaked reinforced specimens. The higher the compaction energy, the higher the difference between the ΔP values of the soaked and unsoaked specimens (Fig. 11). The bearing capacity difference demonstrates the net bearing capacity improvement through the soil-reinforcement interaction, tension membrane mobilized in reinforcement layers and soil density enhancement. The increment in ΔP after soaking would be explained by analyzing the changes of those factors. First, the soil-reinforcement interface shear strength reduced about 13.4% ~ 27.7% from as-compacted conditions to saturated conditions. That reduction induces the decrease in the net bearing capacity improvement (Bergado *et al.* 2006; Chai and Saito 2016). However, as reported by Nguyen *et al.* (2021), the efficiency factor at saturated condition is much higher than that at as-compacted condition. It indicates that a strong interface interaction was maintained to enhance the bearing capacity of the reinforced specimens after saturated. Secondly, the tension membrane in the reinforcement layers of soaked and unsoaked reinforced specimens would be similar as the similar deformation of reinforcement layers observed from tests, presented and analyzed in the next section. Last, as mentioned previously, compared to the unreinforced specimens, the permeable nonwoven geotextile improved the density of the clay in reinforced specimens after compaction. After soaking, the density improvement was further increased due to a strong interface interaction to confine effectively the expansion of the reinforced clay. That also induces the higher bearing capacity difference in the reinforced clay after soaking. To summarize, the bearing capacity difference of the soaked specimens was higher than that of the unsoaked specimens, revealing that the decrement of ΔP (caused by the reduction of the interface shear strength between the soil and reinforcement) was less than its increment (induced through the swelling minimization during soaking).

The CBR values of the specimens before and after soaking clarified this result. The results summarized in Table 4 revealed that the CBR values of the unreinforced clay drastically decreased from 9.5 to 1.5 in the specimen compacted using 486 kJ/m³ of compaction energy after soaking. When the soil density was increased using the highest compaction energy (E = 2,700 kJ/m³), the CBR value of the unreinforced specimen likewise decreased from 40.5 to 3.5 when immersed in water. Lakshmi *et al.* (2016) verified the significant decrement of the CBR value of low-plasticity silty clay after soaking. In particular, after soaking, the CBR of the unsoaked clay decreased from 10 to 20 down to 0.5 to 2.8, depending on the value of E. The excessive loss of the bearing capacity of the unreinforced specimens after soaking reflected the destruction of the soil structure through wetting and swelling.

Conversely, after soaking, the CBR value of the reinforced specimens remained as high as 3.9 to 6.6 for the specimens compacted using the lowest compaction energy (E = 486 kJ/m³). Moreover, the increment of compaction energy induced a significant increment in the CBR value of the reinforced specimen after soaking. Under the highest compaction energy (E = 2,700 kJ/m³), the CBR value of the soaked reinforced specimens increased to 13.5 to 29.6, depending on the number of reinforcement layers. This finding supported the use of nonwoven geotextile reinforced clay under a high compaction energy to achieve a high bearing capacity for both soaked and unsoaked specimens.

3.5 Effect of Soaking on the CBR Behavior

The results revealed that, after soaking, the CBR values of both the unreinforced and reinforced specimens decreased significantly. To evaluate the effect of soaking on reducing the bearing capacity of the clay specimens, the percent CBR reduction after soaking was calculated as follows:

$$\%\Delta CBR = \frac{CBR_{\text{unsoaked}} - CBR_{\text{soaked}}}{CBR_{\text{unsoaked}}} \times 100\% \quad (10)$$

where the CBR_{unsoaked} and CBR_{soaked} represent the CBR value of the unsoaked and soaked specimens, respectively.

Figure 12 depicts the percent CBR reduction of the unreinforced and reinforced specimens after 96 h of soaking. For the unreinforced specimens, their bearing capacity was significantly

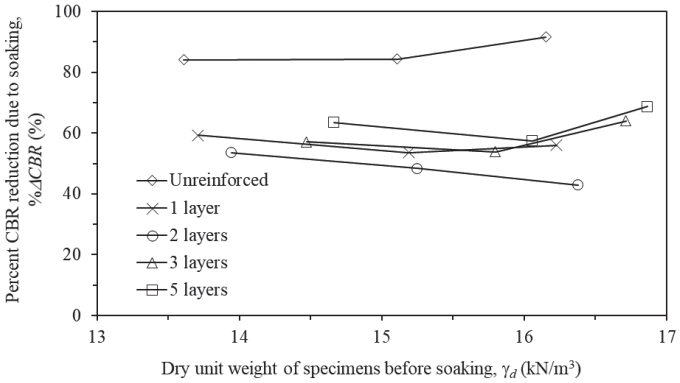

Fig. 12 Percent CBR reduction due to soaking of unreinforced and reinforced specimens

reduced through soaking. In particular, the CBR of the unreinforced specimens decreased approximately 84.1% to 91.7%, equivalent to 6.3 to 12-time reduction. The percent of CBR reduction of the unreinforced soil specimens after soaking increased slightly with an increased compaction energy. The enormous shear strength reduction of clayey soil after soaking has been studied by other researchers. The CBR of low-plasticity silty clay decreased by approximately 86.1% to 95.5% after soaking (Lakshmi *et al.* 2016), and lateritic soil mixed with clay powder exhibited more than an 80% soil strength reduction when soaked (Adam *et al.* 2016).

The strength reduction after soaking was remedied when the nonwoven geotextile layers were applied. As illustrated in Fig. 12, the value of the %Δ*CBR* of the reinforced specimens was approximately 42.9% to 68.8% depending on the number of reinforcement layers and soil density of the specimens prior to soaking. The specimens reinforced with two and five reinforcement layers exhibited the lower and highest CBR reduction, respectively.

The significant reduction in the bearing capacity of the unreinforced and reinforced clay specimens resulted from the wetting and swelling effects when soaking. In unreinforced soil, the wetting effect reduces the friction and cohesion among soil particles resulting in shear strength reduction (Salman 2011; Abdul Samad *et al.* 2018). In the reinforced soil, the wetting effect likewise reduced both the shear strength of the soil and interface shear strength between the reinforcement and soil. In addition, the soil density was reduced as a result of the swelling effect, which also caused the bearing capacity reduction of the specimens.

The influence of the swelling and wetting effects on CBR reduction were analyzed using the relationship between the dry unit weight and CBR of the specimens, as presented in Fig. 13. After soaking, both the CBR value and dry unit weight of the soaked specimens were less than those of the unsoaked specimens. The CBR reduction after wetting $\Delta CBR_{\text{wetting}}$ was defined as the difference between the CBR of the specimens before soaking CBR_{unsoaked} and after soaking without changes to the soil density $CBR_{\text{soaked\_non\_swelling}}$ (Fig. 14).

$$\Delta CBR_{\text{wetting}} = CBR_{\text{unsoaked}} - CBR_{\text{soaked\_non\_swelling}} \quad (11)$$

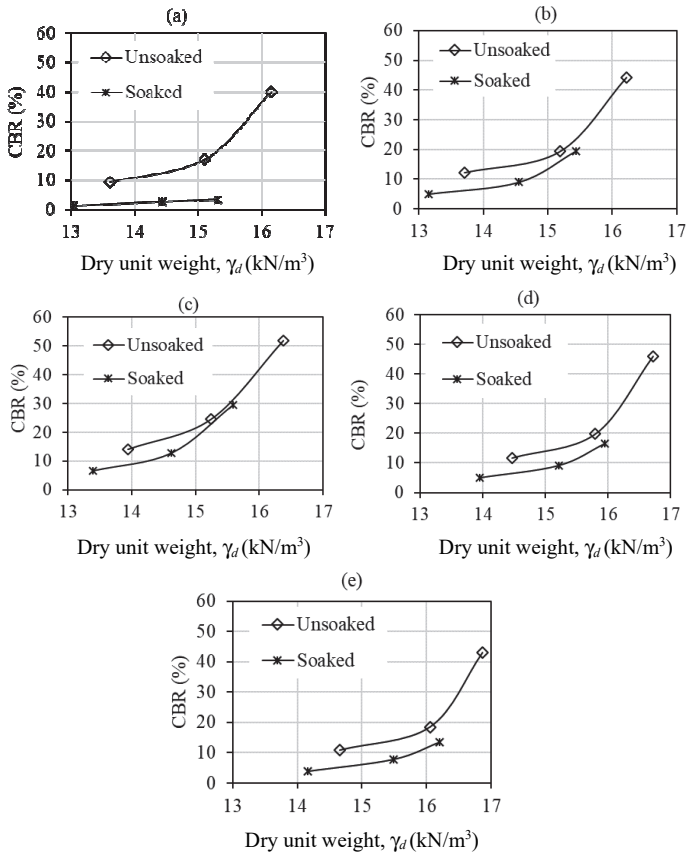

Fig. 13 Variation of CBR with dry unit weights of (a) unreinforced specimens and reinforced specimens with a various number of reinforcement layers: (a) unreinforced; (b) single layer; (c) two layer; (d) three layers; and (e) five layers

The value of the $\Delta CBR_{\text{wetting}}$ was evaluated using two methods. Figure 14 illustrates the measured CBR values of the unsoaked and soaked specimens (*i.e.,* soaking with swelling), denoted by the bold circle and bold triangular nodes, respectively. The CBR value of the soaked specimen without swelling (*i.e.,* the simulated CBR value of the soaked specimen with no density changes) $CBR_{\text{soaked\_non\_swelling}}$ was interpolated using the value of $\gamma_{d\text{-unsoaked}}$, which is indicated by the empty square node in Fig. 14.

The other method involved adopting the measured CBR and dry unit weight of a soaked specimen to be those of a simulated soaked specimen without swelling. Presented as the two points at the same coordination depicted in Fig. 14, the measured and simulated CBR values of a soaked specimen are represented by the bold triangular node and empty rectangular node, respectively. The simulated CBR of the unsoaked specimen was interpolated using the dry unit weight of the simulated soaked specimen, which is indicated by the empty circle. The dry unit weight of the simulated soaked specimens with swelling (*i.e.,* the empty triangular node) was determined through application of the correlation function presented in Fig. 6; finally, its CBR value was interpolated using its dry unit weight estimated in the previous step.

Based on the results of the $\Delta CBR_{\text{wetting}}$, the percent CBR reduction after soaking could be calculated as

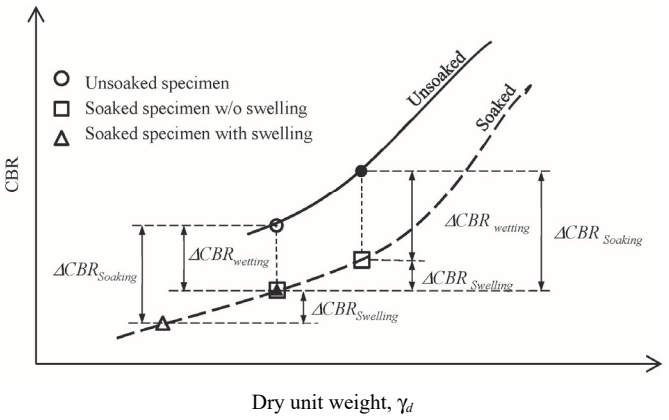

Fig. 14 Evaluation of CBR reduction of specimens due to wetting and swelling effects when soaking. The bold and empty symbols denoted the measured and evaluated values, respectively

$$\%\Delta CBR_{\text{wetting}} = \frac{\Delta CBR_{\text{wetting}}}{CBR_{\text{unsoaked}}} \times 100\% \quad (12)$$

Figure 15 depicts the variation of the $\%\Delta CBR_{\text{wetting}}$ with the dry unit weight of the specimens before soaking. Compared with the percent CBR reduction after soaking illustrated in Fig. 12, the $\%\Delta CBR_{\text{wetting}}$ was smaller, which indicated the lower bearing capacity reduction of specimens soaked without swelling.

The CBR reduction after wetting of the reinforced specimens was smaller than that of the unreinforced specimens (Fig. 15). The $\%\Delta CBR_{\text{wetting}}$ of the unreinforced specimens was approximately 80%, equivalent to an approximate 4-time reduction of the CBR value of the soaked specimen without density changes. Contrarily, the CBR value of the reinforced specimens decreased less than 50% (an approximate 2-time reduction) after wetting. Thus, the higher the soil density, the lower the $\%\Delta CBR_{\text{wetting}}$ value. At the same dry unit weight before soaking, the $\%\Delta CBR_{\text{wetting}}$ of the specimens reinforced with two and five reinforcement layers was the lowest and highest, respectively. Notably, the CBR reduction resulting from wetting could be minimized to only 4.5% when the reinforced specimen was compacted with two reinforcement layers until the dry unit weight of the soil reached as much as 15.6 kN/m^3.

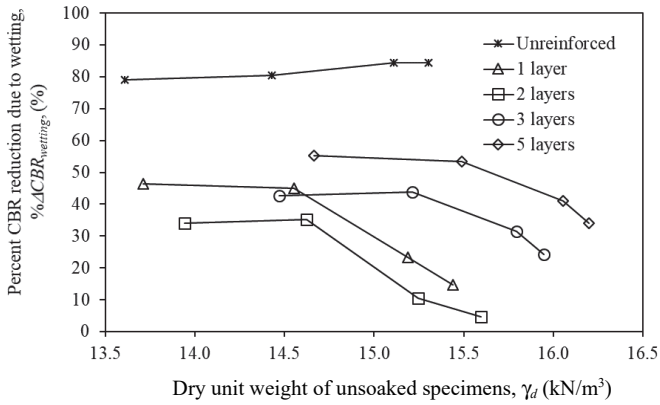

Fig. 15 Percent CBR reduction due to wetting of unreinforced and reinforced specimens

In short, the nonwoven geotextile strengthens the clay after compaction and reduces the loss of bearing capacity after soaking. In addition, the bearing capacity reduction of the reinforced specimen can be further minimized through limiting the expansion of the reinforced specimens during soaking.

CONCLUSIONS

A series of CBR tests was performed to investigate the bearing capacity of riverbed clay specimens reinforced with nonwoven geotextile layers. The results demonstrated that the reinforcing effects serve to improve the bearing capacity of reinforced clay in both soaked and unsoaked conditions. The other conclusions are as follows.

- The permeable reinforcement induces a faster swell through the addition of more drainage paths into the reinforced specimens and reduces the final percent swell and soil density reduction after soaking. The higher the number of reinforcement layers in the reinforced specimens, the lower the percent swell, and the higher the soil density.
- The nonwoven geotextile significantly increased the CBR value of clay under both soaked and unsoaked conditions. The reinforced specimens required sufficient deformation to mobilize the shear strength of the soil-reinforcement interaction and membrane force from the reinforcement tension. When the penetration was less than 10 mm, the specimens reinforced with two reinforcement layers (*i.e., h/D* ≒ 0.8) achieved the highest bearing capacity; when the penetration exceeded 18 mm, the specimens reinforced with more reinforcement layers had a higher bearing capacity.
- The *BCR* of the unsoaked specimens was much smaller than that of the soaked specimens. When the specimens had two reinforcement layers, the *BCR* of the reinforced specimens reached the highest value, which was 1.3 to 1.5 and 4.3 to 8.6 for the unsoaked and soaked specimens, respectively. The increment of the compaction energy increased the *BCR* of the specimens after soaking.
- The bearing capacity improvement of the reinforced clay specimens was a result of the soil-reinforcement interaction, tension membrane and soil density enhancement in both the soaked and unsoaked specimens. The bearing capacity improvement of the soaked specimens was higher than that of the unsoaked specimens, indicating that the reduction of the ΔP induced through the decrease in the interface shear strength between the soil and reinforcement was smaller than the increment of the ΔP induced through the swelling minimization during soaking.
- After soaking, the CBR values of the unreinforced and reinforced specimens decreased significantly. After 96 h of soaking, the CBR of the unreinforced specimens decreased 6.3 to 12 times, and the CBR reduction for the reinforced specimens decreased to less than 70%.
- When absorbing water, the bearing capacity of the specimens was reduced because of the increment in water content (wetting effect) and decrement in density (swelling effect). For the unreinforced specimens, the $\%\Delta CBR_{\text{wetting}}$ value was approximately 80%, decreasing to less than 50% for the reinforced specimens. Notably, only 4.5% of the wetting-induced CBR reduction could be achieved when com-

pacting the reinforced specimens with two reinforcement layers until the dry unit weight of the soil was 15.6 kN/m^3. In short, the bearing capacity reduction of the clayey soil was significantly minimized when the specimens were reinforced with two nonwoven geotextile layers, which promoted expansion restraint during soaking.

Finally, the substantial reduction of the bearing capacity of the unreinforced clay demonstrated the failure potential of unreinforced compacted clay structure after wetting. The bearing capacity reduction of clayey soil can be significantly minimized when the soil is reinforced using a nonwoven geotextile layer in combination with the swelling restraint for the reinforced soil during soaking. The marked reduction of the bearing capacity of the unreinforced and reinforced clay indicated that a functioning drainage system is crucial for ensuring that unreinforced and reinforced clay structures maintain their bearing capacity and stability.

FUNDING

This research is funded by Vietnam National Foundation for Science and Technology Development (NAFOSTED) under grant number 107.01-2016.31.

DATA AVAILABILITY

All data used in this study are included in this paper.

CONFLICT OF INTEREST STATEMENT

The authors declare that there is no conflict of interest.

LIST OF NOTATIONS

a	maximum penetration of piston (m)
B, b	diameter of foundation and piston, respectively (m)
BCR	bearing capacity ratio, (dimensionless)
CBR_1 and CBR_2	CBR value at 2.54 and 5.0mm of corrected penetration, respectively (dimensionless)
CBR_{soaked}, $CBR_{unsoaked}$	CBR value of soaked and unsoaked specimen, respectively (dimensionless)
$CBR_{soaked\_non\_swelling}$	CBR value of the soaked specimen without swelling (dimensionless)
d_i	is the depth of the geotextile layer i in the specimens (m)
D, H	diameter and height of mold, respectively (m)
E	compaction energy (J/m^3)
H_{soil}	height of soil only before soaking (m)
h	reinforcement spacing (m)
i,n	ordinal number and total number of reinforcement layers in reinforced specimens, respectively (dimensionless)
k	cross-plane permeability geotextile (m/s)
P_1, P_2	stress on piston at 2.54 mm and 5.08 mm of corrected penetration, respectively (N/m^2)
$q_{overburden}$	overburden pressure (N/m^2)
R_f	efficiency factor (dimensionless)
R_δ	maximum deflection ratio (dimensionless)
R^2	coefficient of determination (dimensionless)
s	vertical swell (m)
S, S_{96}.	percent swell with time and after 96 h of soaking (dimensionless)
t_i, t_{min}, t_{max}	actual, minimum, and maximum thickness of a geotextile layer, respectively (m)
V	volume of mold (m^3)
W, W_{re}	moisture weight of unreinforced specimens and reinforced specimens, respectively, (N)
W^d_{soil}	total weight of dry soil (N)
W_{geo}	dry weight of geotextile layers (N)
$\%\Delta\gamma_d$	percentage of dry unit weight reduction (dimensionless)
$\%\Delta CBR$	percent CBR reduction due to soaking (dimensionless)
$\%\Delta CBR_{wetting}$	percent of CBR reduction due to wetting (dimensionless)
ω	water content of soil specimens (dimensionless)
$\sigma_{\gamma d\text{-re}}$	standard deviation of the dry unit weight of reinforced soil (dimensionless)
γ, γ_d	bulk and dry unit weight of soil, respectively (N/m^3)
$\gamma_{d\_unsoaked}$, γ_{d_soaked}	dry unit weight of soil in unsoaked and soaked specimens, respectively (N/m^3)
$\gamma_{d\text{-unre}}$, $\gamma_{d\text{-re}}$	dry unit weight of unreinforced and reinforced specimens, respectively (N/m^3)
$\Delta CBR_{wetting}$	CBR reduction due to wetting (dimensionless)
σ_{ti}	standard deviation of the geotextile thickness (dimensionless)
ψ	permittivity (s^{-1})

REFERENCES

AASHTO (1993). *Guide for Design of Pavement Structures*. American Association of State Highway and Transportation Officials, Washington, D.C.

Abdul Samad, A.R., Norbaya, S., Juhaizad, A., Hazwani, M.Z., and Ikmal F.R. (2018). "Shear strength behavior for unsoaked and soaked multistage triaxial drained test." *Advancements in Civil Engineering & Technology*, **1**(4), 96-101. https://dx.doi.org/10.31031/acet.2018.01.000518

Abduljauwad, S.N., Bayomy, F., Al-Shaikh, A.M., and Al-Amoudi, O.S.B. (1994). "Influence of geotextiles on performance of saline sebkha soils." *Journal of Geotechnical Engineering*, ASCE, **120**(11), 1939-1960. https://doi.org/10.1061/(ASCE)0733-9410(1994)120:11(1939)

Abu-Farsakh, M., Coronel, J., and Tao, M. (2007). "Effect of soil moisture content and dry density on cohesive soil-geosynthetic interactions using large direct shear tests." *Journal of Materials in Civil Engineering*, ASCE, **19**(7),

540-549. https://doi.org/10.1061/(ASCE)0899-1561(2007)19:7(540)

Adams, C.A., Tuffour, Y.A., and Kwofie, S. (2016). "Effects of soil properties and geogrid placement on CBR enhancement of lateritic soil for road pavement layers." *American Journal of Civil Engineering and Architecture*, **4**(2), 62-66. https://doi.org/10.12691/ajcea-4-2-4

Al-Taie, A., Disfani, M.M., Evans, R., Arulrajah, A., and Horpibulsuk, S. (2016). "Swell-shrink cycles of lime stabilized expansive subgrade." *Procedia Engineering*, **143**, 615-622. https://doi.org/10.1016/j.proeng.2016.06.083

ASTM D 1557: *Test Methods for Laboratory Compaction Characteristics of Soil Using Modified Effort (56,000 ft-lbf/ft3(2,700 kN-m/m^3)*. ASTM International, West Conshohocken, PA, USA. https://doi.org/10.1520/D1557-07

ASTM D 1883: *Standard Test Method for California Bearing Ratio (CBR) of Laboratory-Compacted Soils.* ASTM International, West Conshohocken, PA, USA. https://doi.org/10.1520/D1883-05

Bergado, D., Ramana, G., Sia, H., and Varun. (2006). "Evaluation of interface shear strength of composite liner system and stability analysis for a landfill lining system in Thailand." *Geotextiles and Geomembranes*, **24**(6), 371-393. https://doi.org/10.1016/j.geotexmem.2006.04.001

Carlos, D.M., Pinho-Lopes, M., and Lopes, M.L. (2016). "Effect of geosynthetic reinforcement inclusion on the strength parameters and bearing ratio of a fine soil." *Procedia Engineering*, **143**, 34-41. https://doi.org/10.1016/j.proeng.2016.06.005

Chai, J.C. and Saito, A. (2016). "Interface shear strengths between geosynthetics and clayey soils." *International Journal of Geosynthetics and Ground Engineering*, **2**(19), (2006). https://doi.org/10.1007/s40891-016-0060-8

Chakraborty, M. and Kumar, J. (2014). "Bearing capacity of circular foundations reinforced with geogrid sheets." *Soils and Foundations*, **54**(4), 820-832. https://doi.org/10.1016/j.sandf.2014.06.013

Chen, J. and Yu, S. (2011). "Centrifugal and numerical modeling of a reinforced lime-stabilized soil embankment on soft clay with wick drains." *International Journal of Geomechanics*, **11**(3), 167-173. https://doi.org/10.1061/(ASCE)GM.1943-5622.0000045

Chen, Q. and Abu-Farsakh, M. (2015). "Ultimate bearing capacity analysis of strip footings on reinforced soil foundation." *Soils and Foundations*, **55**(1), 74-85. https://doi.org/10.1016/j.sandf.2014.12.006

Choudhary, A., Gill, K., Jha, J., and Shukla, S.K. (2012). "Improvement in CBR of the expansive soil subgrades with a single reinforcement layer." *Proceedings of Indian Geotechnical Conference*, Indian Geotechnical Society, New Delhi, India, 289-292.

Fourie, A.B. and Fabian, K.J. (1987). "Laboratory determination of clay geotextile interaction." *Geotextiles and Geomembranes*, **6**(4), 275-294. https://doi.org/10.1016/0266-1144(87)90009-4

Giroud, J.P. and Noiray, L. (1981). "Geotextile-reinforced unpaved roads." *Journal of the Geotechnical Engineering Division*, ASCE, **107**(9), 1233-1254. https://doi.org/10.1061/AJGEB6.0001187

Holtz, R.D., Kovacs, W.D., and Sheahan, T.C. (2011). *An Introduction to Geotechnical Engineering*, 2nd Edition, Pearson Education, Inc., Upper Saddle River, New Jersey.

Indraratna, B., Satkunaseelan, K.S., and Rasul, M.G. (1991). "Laboratory properties of a soft marine clay reinforced with woven and nonwoven geotextiles." *Geotechnical Testing Journal*, GTJODJ, **14**(3), 288-295. https://doi.org/10.1520/GTJ10573J

Ingold, T.S. and Miller, K.S. (1982). "The performance of impermeable and permeable reinforcement in clay subject to undrained loading." *Quarterly Journal of Engineering Geology and Hydrogeology*, **15**(3), 201-208. https://doi.org/10.1144/GSL.QJEG.1982.015.03.03

IS: *1498 Classification and Identification of Soils for General Engineering Purposes*. Bureau of Indian Standards, New Delhi, India

IS: *2720-40 Methods of Test for Soils, Part 40: Determination of Free Swell Index of Soils*. Indian Standard Methods of Test for Soils, New Delhi, India

ISO 9863-1:2016(E) *Geosynthetics—Determination of Thickness at Specified Pressures—Part 1: Single Layers*. International Standard, Switzerland

Kamel, M.A., Chandra, S., and Kumar, P. (2004). "Behaviour of subgrade soil reinforced with geogrid." *International Journal of Pavement Engineering*, **5**(4), 201-209. https://doi.org/10.1080/1029843042000327122

Keerthi, N. and Kori, S. (2018). "Study on improvement of sub grade soil using soil-reinforcement technique," *International Journal of Applied Engineering Research*, **13**(7), 126-134. https://doi.org/10.37622/000000

Keskin, S.N., Cimen, O., Goksan, T.S., Uzundurukan, S., and Karpuzcu, M. (2009). "Effect of geotextiles on the compaction properties of soils." *Proceedings of 2nd International Conference on New Developments in Soil Mechanics and Geotechnical Engineering*, Near East University, Nicosia, North Cyprus, 420-424.

Koerner, R.M. and Narejo, D. (1995). "Bearing capacity of hydrated geosynthetic clay liners." *Journal of Geotechnical and Geoenvironmental Engineering*, ASCE, **121**(1), 82-85. https://doi.org/10.1061/(ASCE)0733-9410(1995)121:1(82).

Kumar, A. and Saran, S. (2003). "Bearing capacity of rectangular footing on reinforced soil." *Geotechnical and Geological Engineering*, **21**(3), 201-224. https://doi.org/10.1023/A:1024927810216

Khemissa, M., Mekki, L., and Mahamedi, A. (2018). "Laboratory investigation on the behaviour of an overconsolidated expansive clay in intact and compacted states." *Transportation Geotechnics*, **14**, 157-168. https://doi.org/10.1016/j.trgeo.2017.12.003

Lake, C.G. and Rowe, R.K. (2000). "Swelling characteristics of needle punched, thermally treated geosynthetic clay liners." *Geotextiles and Geomembranes*, **18**(2-4), 77-101. https://doi.org/10.1016/S0266-1144(99)00022-9

Lakshmi, S.M., Subramanian, S., Lalithambikhai, M.P., Vela, A.M., and Ashni, M. (2016). "Evaluation of soaked and unsoaked CBR values of soil based on the compaction characteristics." *Malaysian Journal of Civil Engineering*, **28**(2), 172-182. https://doi.org/10.11113/mjce.v28.15712

Malizia, J.P. and Shakoor, A. (2018). "Effect of water content and density on strength and deformation behavior of clay soils." *Engineering Geology*, **244**, 125-131. https://doi.org/10.1016/j.enggeo.2018.07.028

Mirzababaei, M., Miraftab, M., Mohamed, M., and McMahon, P. (2013). "Unconfined compression strength of reinforced clays with carpet waste fibers." *Journal of Geotechnical and Geoenvironmental Engineering*, ASCE, **139**(3), 483-493. https://doi.org/10.1061/(ASCE)GT.1943-5606.0000792

Mitchell, J.K. and Soga, K. (2005). *Fundamentals of Soil*

Behavior. 3rd Edition, John Wiley and Sons, 577 p.

Moghaddas-Nejad, F. and Small, J.C. (1996). "Effect of geogrid reinforcement in model track tests on pavements." *Journal of Transportation Engineering*, ASCE, **122**(6), 468-474. https://doi.org/10.1061/(ASCE)0733-947X(1996)122:6(468)

NCHRP (2004). *Guide for Mechanistic-Empirical Design of New and Rehabilitated Pavement Structures*. National Cooperative Highway Research Program 1-47A Report. Transportation Research Board, National Research Council, Washington, DC.

Noorzad, R. and Mirmoradi, S.H. (2010). "Laboratory evaluation of the behavior of a geotextile reinforced clay." *Geotextiles and Geomembranes*, **28**(4), 386-392. https://doi.org/10.1016/j.geotexmem.2009.12.002

Nguyen, M.D. and Ho, M.P. (2021). "The influence of saturation on the interface shear strength of clay and nonwoven geotextile." *Journal of Science and Technology in Civil Engineering (STCE) - NUCE*, **15**(1), 41-54. https://doi.org/10.31814/stce.nuce2021-15(1)-04

Nguyen, M.D., Yang, K.H., and Yalew, W.M. (2020). "Compaction behavior of nonwoven geotextile-reinforced clay." *Geosynthetics International*, **27**(1), 16-33. https://doi.org/10.1680/jgein.19.00053

Nguyen, M.D., Yang, K.H., Lee, S.H., Wu, C.S., and Tsai, M.H. (2013). "Behavior of nonwoven geotextile-reinforced sand and mobilization of reinforcement strain under triaxial compression." *Geosynthetics International*, **20**(3), 207-225. https://doi.org/10.1680/gein.13.00012

Rajesh, U., Sajja, S., and Chakravarthi, V.K. (2016). "Studies on engineering performance of geogrid reinforced soft subgrade." *Transportation Research Procedia*, **17**, 164-173. https://doi.org/10.1016/j.trpro.2016.11.072

Salman, A.D. (2011). "Soaking effects on the shear strength parameters and bearing capacity of soil." *Engineering and Technology Journal*, **29**(6), 1107-1123. https://doi.org/10.47191/etj

Singh M., Trivedi, A., and Shukla, S.K. (2019). "Strength enhancement of the subgrade soil of unpaved road with geosynthetic reinforcement layers." *Transportation Geotechnics*, **19**, 54-60. https://doi.org/10.1016/j.trgeo.2019.01.007

Spangler, M.F. and Handy, R.L. (1973). *Soil Engineering.* 3rd Edition, Intest Educational Publishers, New York, NY.

Sridharan, A. and Gurtug, Y. (2004). "Swelling behaviour of compacted fine-grained soils." *Engineering Geology*, **72**(1-2), 9-18. https://doi.org/10.1016/S0013-7952(03)00161-3

Sridharan, A., Murthy, B.R.S., and Revanasiddappa, K. (1991). "Technique for using fine-grained soil in reinforced earth." *Journal of Geotechnical Engineering*, ASCE, **117**(8), 1174-1190. https://doi.org/10.1061/(ASCE)0733-9410(1991)117:8(1174)

Taechakumthorn, C. and Rowe, R. (2012). "Performance of reinforced embankments on rate-sensitive soils under working conditions considering effect of reinforcement viscosity." *International Journal of Geomechanics*, ASCE, **12**(4), 381-390. https://doi.org/10.1061/(ASCE)GM.1943-5622.0000094

Wang, J.Q., Zhang, L.L., Xue, J.F., and Tang, Y. (2018). "Load-settlement response of shallow square footings on geogrid-reinforced sand under cyclic loading." *Geotextiles and Geomembranes*, **46**(5), 586-596. https://doi.org/10.1016/j.geotexmem.2018.04.009

Yang, K.H., Nguyen, M.D., Yalew, W.M., Liu, C.N., and Gupta, R. (2016). "Behavior of geotextile-reinforced clay under consolidated-undrained tests: Reinterpretation of porewater pressure parameters." *Journal of GeoEngineering*, **11**(2), 45-57. http://dx.doi.org/10.6310/jog.2016.11(2).1

Yang, K.H., Yalew, W.M., and Nguyen, M.D. (2015). "Behavior of geotextile-reinforced clay with a coarse material sandwich technique under unconsolidated-undrained triaxial compression." *International Journal of Geomechanics*, ASCE, **16**(3), GM.1943-5622.0000611. https://doi.org/10.1061/(ASCE)GM.1943-5622.0000611

Yetimoglu, T., Wu, J.T.H., and Saglamer, A. (1994). "Bearing capacity of rectangular footings on geogrid-reinforced sand." *Journal of Geotechnical Engineering*, ASCE, **120**(12), 2083-2099. https://doi.org/10.1061/(ASCE)0733-9410(1994)120:12(2083)

Zornberg, J.G. and Mitchell, J.K. (1994). "Reinforced soil structures with poorly draining backfills, Part I: Reinforcement interactions and functions." *Geosynthetics International*, **1**(2), 103-148. https://doi.org/10.1680/gein.2.0011